Capillary Neutron Lens for Prompt Gamma Activation Micro-Analysis

Glass polycapillary fibers with hundreds of hollow micrometer-wide channels have been used for guiding and changing the direction of slow neutrons [1]. The use of a monolithic lens to focus neutron beams for prompt-gamma activation analysis (PGAA) of small samples has been explored earlier [2]. In addition, the converging nature of a focused beam can provide magnified images for neutron radiography [3]. We have combined these two uses of the focused beam from a monolithic lens and have implemented an alignment procedure for PGAA aided by neutron imaging.

The measurements have been performed at the end of the NG-0 beam line at the NCNR [4]. The average wavelength of the incident beam with a Be filter is about 0.6 nm. Neutrons are imaged with a camera that consists of a ZnS(Ag)/^{6}LiF scintillator coupled with a CCD camera with an average pixel size of 50 µm. The gamma-ray spectrometry system [5] consists of a p-type germanium photon detector with a virtual pulser "loss free" counting module. The two monolithic lenses used in this study are both fabricated from a bundle of capillaries that is 50 mm long and with a hexagonal cross section 10 mm wide (flat-to-flat) at the entrance and tapered to 3 mm at exit. The distance from the exit to the focus is 8.8 mm for lens A and 9.8 mm for lens B. Each lens is installed on *x*-*y*-*z* translation stages with two directions of tilt motion. The experimental layout is shown schematically in Fig. 1.

An optimum focal spot from lens A is recorded with the imaging detector. Line profiles across the focal spot in both the horizontal and vertical directions are taken to determine the intensity distribution and the FWHM (H: 87 µm, V: 100 µm) of the focus (Fig. 2 a). The gain in neutron current density within the 100 µm x 100 µm area is 46 ± 2, and within a 50 µm x 50 µm area it is 71 ± 5. Images and their sizes and intensity as a function of *z* are shown in Fig. 2b.

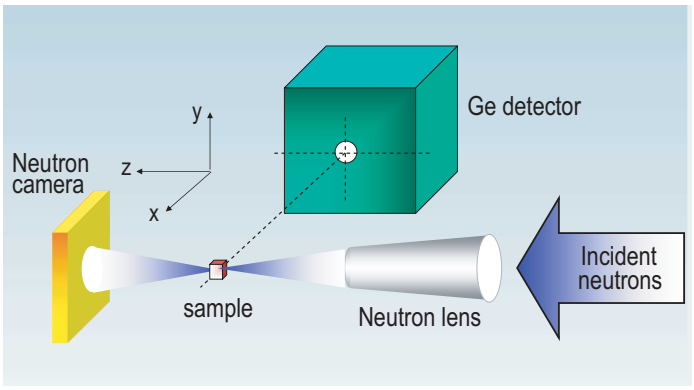

FIGURE 1. Schematic experimental layout.

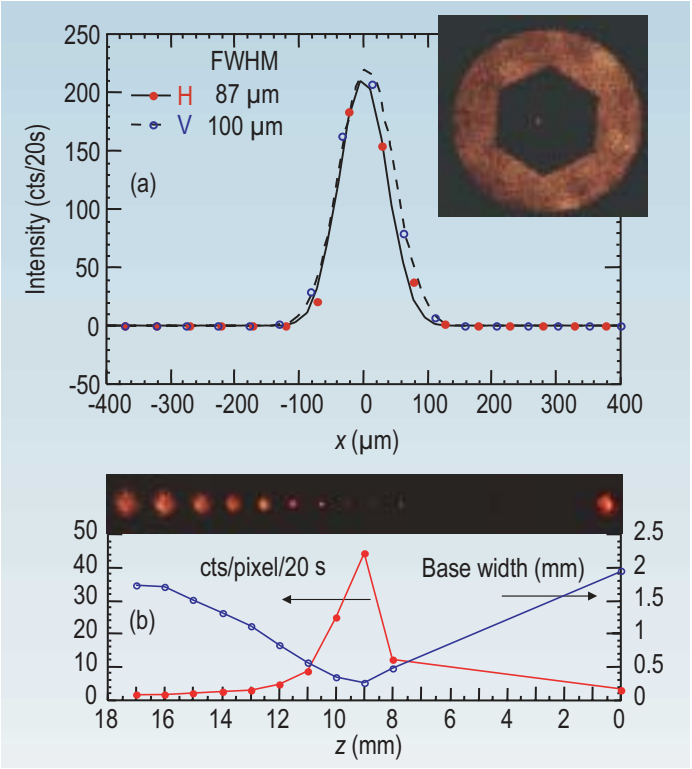

FIGURE 2. (a) Line profiles of the focal spot intensity in the horizontal and vertical directions. Insert: Focused beam image – the focus is near the center of the hexagonal shadow cast by the lens entrance surrounded by the background of unguided neutrons. (b) Intensity and base width of the spot along the beam path, and images of the focused beam "foot print." A linear fit to the region between 10 mm and 16 mm gives a slope of 0.233 radians, or a 13.3° convergence angle.

The focused beam creates a neutron "point source," with neutrons departing the focus within a cone of about 13°. Any neutron-absorbing object within the path of the divergent beam will cast a magnified shadow at some further distance. We make use of this effect in order to align a small sample, a Gd foil (thickness 25 µm) of size 2 mm x 0.9 mm, at the focus for PGAA (Fig. 3a). We vary the distance L_1 between the sample and the lens focus by translating the lens

H. H. Chen-Mayer, G. P. Lamaze,
D. F. R. Mildner and R. Zeisler
NIST Center for Neutron Research, and
Analytical Chemistry Division
Chemical Science and Technology Laboratory
National Institute of Standards and Technology
Gaithersburg, MD 20899-8395

W. M. Gibson
X-Ray Optical Systems, Inc.
Albany, NY 12203

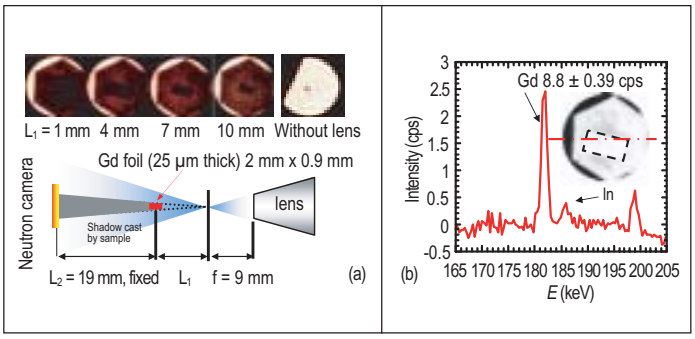

FIGURE 3. (a) Magnified image of the sample at various values of L_1. The image of the sample without the lens is also shown for comparison. (b) Prompt gamma spectrum for Gd (182 keV) and for In (186 keV) measured with the lens, and the corresponding image of the sample.

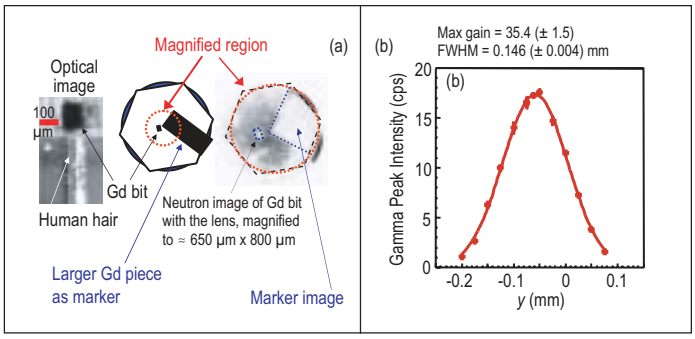

FIGURE 4. (a) Optical image of the Gd piece in comparison with a strand of human hair (left), and neutron image using lens B. The large solid rectangle is a larger Gd strip marker to help locate the smaller sample more easily. (b) Gd peak intensity produced by a y-scan of the lens.

along the direction of the beam. The magnified image enables a better alignment of the sample with respect to the focus. From the earlier measurement of the lens focal point (Fig. 2), we determine the location of the focus with respect to the large hexagonal shadow cast by the lens entrance. We then move the lens transversely such that the image of the sample is now superimposed on the image of the focal point. This guarantees that the focal point is indeed on the sample. Once the image is centered, the lens is translated to $L_1 = 0$ such that the focus is on the sample, ready for prompt gamma measurements.

At the center of the same Gd sample described above, there is an additional indium foil of about 1 mm x 1 mm in cross section, in contact with the Gd strip. The prompt gamma measurement without the lens gives a peak intensity for Gd at 182 keV of 2.1 counts per second (cps), but the In peak at 186 keV is not visible even for a 20 min measurement. When the lens is used in a 10 min measurement, not only has the Gd peak intensity increased, but the In peak has also become visible (Fig. 3b). Since the Gd piece is much larger than the focal spot size, the gain in sensitivity for Gd is only a factor of 4. The gain for In is not estimated.

We have also used lens B for an even smaller sample, a Gd piece of 128 μm x 103 μm x 25 μm in size and 2.59 μg in mass (effective mass ≈ 1 μg taking into account self-absorption). The images from an optical microscope and from neutron measurements are shown in Fig. 4a. Without the lens, the neutron camera cannot resolve the 100 μm particle. The gamma intensity with the lens is 17.4 cps with a 1.6 % 1σ counting statistics after 1 hour of counting, and with the direct beam 0.506 cps (3.9 % 1σ) after 19.5 hours. The gain, given by the ratio of the two count rates, is 34 ± 1.4. A scan of the lens in the vertical direction yields a peak, given by the convolution of the sample width with the beam width, as shown in Fig. 4b. The FWHM of the peak is 148 (± 1.5) μm, correctly corresponding to the 100 μm sample-width and the 100 μm beam-width added in quadrature.

The effort presented here is a step toward providing quantitative elemental information to traditional neutron radiography. This new tool will provide a unique capability in non-destructive analysis for industrial materials. In the future, the system will be automated to scan, giving a more efficient probe for microanalysis with neutron beams.

References

[1] M. A. Kumahkov and V. A. Sharov, Nature 357, 390 (1992), and H. Chen, R. G. Downing, D. F. R. Mildner, W. M. Gibson, M. A. Kumakhov, I. Yu. Ponomarev, and M. V. Gubarev, Nature **357**, 391 (1992).

[2] V. A. Sharov, Q. F. Xiao, I. Yu. Ponomarev, D. F. R. Mildner, and H. H. Chen-Mayer, Rev. Sci. Instrum. **71**, 3247 (2000).

[3] K. M. Podurets, D. F. R. Mildner, and V. A. Sharov, Rev. Sci. Instrum. **69**, 3541 (1998).

[4] D. F. R. Mildner, H. H. Chen-Mayer, G. P. Lamaze, and V. A. Sharov, Nucl. Instrum. & Meth. A**413**, 341 (1998).

[5] R. Zeisler, G. P. Lamaze, H. H. Chen-Mayer, J. Radioanal. Nucl. Chem. **248**, 35 (2001).